Biochemistry

© Copyright 1998 by the American Chemical Society Volume 37, Number 30 July 28, 1998

Accelerated Publications

Hydrogen Bonding of Redox-Active Tyrosine Z of Photosystem II Probed by FTIR Difference Spectroscopy†

Catherine Berthomieu,*,‡ Rainer Hienerwadel,‡,§ Alain Boussac,‡ Jacques Breton,‡ and Bruce A. Diner||

CEA-Saclay, Section de Bioénergétique, 91 191 Gif-sur-Yvette, Cedex, France, and Central Research and Development Department, Experimental Station, E. I. du Pont de Nemours & Co., Wilmington, Delaware 19880-0173

Received April 8, 1998; Revised Manuscript Received May 28, 1998

ABSTRACT: The $Tyr_Z^{\bullet}/Tyr_Z$ FTIR difference spectrum is reported for the first time in Mn-depleted photosystem II (PS II)-enriched membranes of spinach, in PS II core complexes of *Synechocystis* sp. PCC 6803 WT, and in the mutant lacking Tyr_D (D2-Tyr160Phe). In *Synechocystis*, the $\nu_{7'a}$(CO) and δ(COH) infrared modes of Tyr_Z are proposed to account at 1279 and 1255 cm^{-1}. The frequency of these modes indicate that Tyr_Z is protonated at pH 6 and involved in a strong hydrogen bond to the side chain of a histidine, probably D1-His190. A positive signal at 1512 cm^{-1} is assigned to the ν(CO) mode of $Tyr_Z^{\bullet}$ on the basis of the 27 cm^{-1} downshift observed upon ^{13}C-Tyr labeling at the Tyr ring C4 carbon. A second IR signal, at 1532 cm^{-1}, is tentatively assigned to the ν_{8a}(CC) mode of $Tyr_Z^{\bullet}$. The frequency of the ν(CO) mode of $Tyr_Z^{\bullet}$ at 1512 cm^{-1} is comparable to that observed at 1513 cm^{-1} for the $Tyr^{\bullet}$ obtained by UV photochemistry of tyrosinate in solution, while it is higher than that of $Tyr_D^{\bullet}$ in WT PS II at 1503 cm^{-1} and that of non-hydrogen-bonded $Tyr_D^{\bullet}$ in the D2-His189Gln mutant at 1497 cm^{-1} [Hienerwadel, R., Boussac, A., Breton, J., Diner, B. A., and Berthomieu, C. (1997) *Biochemistry 36*, 14712−14723]. This latter work and the present FTIR study suggest that hydrogen bonding induces an upshift of the ν(CO) IR mode of tyrosyl radicals and that $Tyr_Z^{\bullet}$ forms (a) stronger hydrogen bond(s) than $Tyr_D^{\bullet}$ in WT PS II. Alternatively, the frequency difference between $Tyr_Z^{\bullet}$ and $Tyr_D^{\bullet}$ ν(CO) modes could be explained by a more localized positive charge near the tyrosyl radical oxygen of $Tyr_D^{\bullet}$ than $Tyr_Z^{\bullet}$. The $Tyr_Z^{\bullet}/Tyr_Z$ spectrum obtained in Mn-depleted PS II membranes of spinach shows large similarities with the S_3'/S_2' spectrum characteristic of radical formation in Mn-containing but Ca^{2+}-depleted PS II, in support of the assignment using ESEEM of $Tyr_Z^{\bullet}$ as being responsible for the split EPR signal observed upon illumination in these conditions [Tang, X.-S., Randall, D. W., Force, D. A., Diner, B. A., and Britt, R. D. (1996) *J. Am. Chem. Soc. 118*, 7638−7639]. The peak at 1514 cm^{-1} is assigned to the ν(CO) mode of $Tyr_Z^{\bullet}$ in these preparations, which indicates that Mn depletion only very slightly perturbs the immediate environment of $Tyr_Z^{\bullet}$ phenoxyl.

Photosystem II (PS II)[1] of plants and cyanobacteria is the site of light-induced oxidation of water to molecular oxygen. A tyrosine (Tyr_Z, D1-Tyr161) of the D1 polypeptide of PS II is a redox intermediate between the chlorophylls that constitute the primary donor of PS II (P_{680}) and the Mn cluster responsible for water oxidation. Models have been recently presented in which Tyr_Z is directly involved in proton or hydrogen atom abstraction from water (*1*−*6*). There is a second redox-active tyrosine (Tyr_D) on the homologous polypeptide D2 of PS II that forms a dark stable neutral

† R.H. was supported by an EC Fellowship (ERB40016T933365).

* Corresponding author. Fax: 00 33 1 69 08 87 17. Tel: 00 33 1 69 08 45 87. E-mail: berthomieu@dsvidf.cea.fr.

‡ CEA-Saclay.

S0006-2960(98)00788-0 CCC: $15.00 © 1998 American Chemical Society
Published on Web 07/10/1998

radical with unknown function (see ref *7* for a review). The two radicals have different redox potentials, the midpoint potential of $Tyr_Z^{\bullet}/Tyr_Z$ being higher than that of $Tyr_D^{\bullet}/Tyr_D$ by approximately 240 mV (*8, 9*). They also differ in their accessibility to exogenous reductants. The structural and environmental factors that explain the different properties of the two radicals are under investigation. It was proposed that the radicals differ in the rigidity of their aromatic ring with respect to the tyrosine alkyl chain (*2*−*4*). In wild-type PS II, $Tyr_D^{\bullet}$ is hydrogen bonded to the side chain of D2-His189 *(10*−*17*), while a tyrosyl radical free from hydrogen bond interaction is observed in the PS II mutant, D2-His189Gln (*15*−*17*). $Tyr_Z^{\bullet}$ is also hydrogen bonded (*1, 12, 14, 15, 18, 19*). The properties of this hydrogen bond differ however from that formed with $Tyr_D^{\bullet}$ (*19*), and the hydrogen bond donor(s) to $Tyr_Z^{\bullet}$ is (are) yet to be identified, though kinetic (*20*−*21*) and structural (*13, 22, 23*) arguments have implicated the homologous D1-His190.

FTIR difference spectroscopy of a light-induced reaction is a method allowing the investigation of structures and interactions at the molecular or atomic level (reviewed in refs *24* and *25*). We have previously identified the IR modes of Tyr_D and $Tyr_D^{\bullet}$ using PS II samples from WT and the D2-His189Gln mutant of *Synechocystis* sp. PCC 6803 with unlabeled or specifically labeled tyrosines (*26, 27*). In this paper, we report the $Tyr_Z^{\bullet}/Tyr_Z$ FTIR difference spectrum obtained both with Mn-depleted PS II-enriched membranes of spinach and with PS II cores of *Synechocystis* sp. PCC 6803. In the latter spectrum, IR modes of Tyr_Z and notably the ν(CO) mode of $Tyr_Z^{\bullet}$ are identified using PS II with specifically ^2H- and ^{13}C-labeled tyrosines. The hydrogen bonding pattern to $Tyr_Z^{\bullet}$ is discussed both in Mn-containing and Mn-depleted PS II by comparison with $Tyr_D^{\bullet}$ and with the tyrosyl radical ($Tyr^{\bullet}$) obtained in solution by UV irradiation.

MATERIALS AND METHODS

Mn-depleted PS II core complexes were isolated according to Rögner et al. (*28*) with the modifications described in Tang et al. (*18*) from the glucose-tolerant (*29*) and phycocyanin-deficient "olive" strain (*28*) of the cyanobacterium *Synechocystis* sp. PCC 6803 wild type (WT) or D2-Tyr160Phe mutant. The isolation of the mutant was previously described (*15, 18*). For the specific labeling of tyrosines, the cyanobacteria were grown photoautotrophically for 6−7 days in BG-11 medium (*30*) containing 0.5 mM phenylalanine, 0.25 mM tryptophan, and 0.25 mM isotopically labeled tyrosine, according to the method of Barry and Babcock (*31*). Control PS II preparations were made from cyanobacteria grown in the presence of unlabeled aromatic amino acids. The $^{13}C_1$-(4)-, $^{13}C_6$-, and $^2H_4$-Tyr (98% isotope enriched) were purchased from Cambridge Isotope Laboratories.

For the FTIR investigation of $Tyr_Z^{\bullet}/Tyr_Z$, a concentrated suspension of PS II cores (at ≈5 mg of Chl/mL) was diluted about 80−100 times in 400 μL of Mes buffer (50 mM), pH 6, containing 10 mM NaCl and 5 mM $MgCl_2$. The suspension was concentrated to about 7 μL using a microcon 30 (Amicon) and deposited onto a CaF_2 window. Sorbitol (0.5 μL of a 0.2 M solution) and ferricyanide (2 μL of a 0.5 M solution) were added to the concentrated PS II solution before partial drying under a N_2-gas stream.

The IR sample was thermostated at −8 °C in a N_2-cooled cryostat in the FTIR spectrometer. IR absorption of the sample was recorded during 3.6 s (20 scans) before and 1 s after a 0.7-s illumination with red light (Xe lamp with water, heat-removing, and a RG 645 nm cutoff filter). The acquisitions were cycled during 8−10 h, with dark periods of 45 s between successive illuminations. Spectra obtained from 6 to 15 samples were averaged. The FTIR spectra were recorded with 4 cm^{-1} resolution on a Bruker IFS 88 spectrometer equipped with a MCT-A detector.

RESULTS

$Tyr_Z^{\bullet}/Tyr_Z$ FTIR Difference Spectrum. The FTIR difference spectrum A of Figure 1 was obtained using PS II cores of the D2-Tyr160Phe site-directed mutant of *Synechocystis* sp. PCC lacking Tyr_D. The sample was maintained at −8 °C in Mes buffer at pH 6 in the presence of ferricyanide. In these experimental conditions, it has been shown by UV−Vis spectroscopy that a $Tyr_Z^{\bullet}/Tyr_Z$ difference spectrum free of Chl^+ or Q_A^- contributions is obtained 600 ms after flash illumination (*32*). A decay halftime of about 5 s was measured at 245 nm for $Tyr_Z^{\bullet}$, while Q_A^-, measured at 325 nm, is fully reoxidized within 1 s after the flash (*32*). In the present FTIR experiments, a short illumination of 0.7 s was used instead of a flash. To avoid IR contributions from Q_A^-/Q_A to the FTIR difference spectrum A of Figure 1, the absorption of the sample was recorded during 3.6 s just before and 1 s after illumination. The inset of Figure 1A shows the 2200−1900 cm^{-1} frequency region of spectrum A. The negative band at 2116 cm^{-1} and the positive one at 2040 cm^{-1} are assigned to ferricyanide and ferrocyanide, respectively. These signals show that ferricyanide acts as electron acceptor upon photochemistry of PS II. It has been shown previously that the Q_A^-/Q_A FTIR spectrum is characterized notably by a strong absorption of the semiquinone at 1478 cm^{-1} with a broad shoulder at 1456 cm^{-1} (*26, 33*−*37*). In the 1800−1000 cm^{-1} region, spectrum A of Figure 1 is very different from the Q_A^-/Q_A FTIR difference spectra mentioned above, and the signal at 1478 cm^{-1} is absent. This confirms that spectrum A in Figure 1 is free of vibrational contributions of the electron acceptor side of PS II.

The electron donor components other than $Tyr_Z^{\bullet}$ that could potentially contribute in Figure 1A are Chl^+ and/or P_{680}^+. Figure 1B shows the spectrum obtained under continuous illumination at −8 °C of Mn-depleted PS II cores of the mutant lacking Tyr_D. In this spectrum, both signals due to the oxidation of P_{680} and of secondary donor Chl(s) are expected to contribute. Spectrum B shows large similarities with the P_{680}^+/P_{680} *(38)* and the Chl^+/Chl (*39*) FTIR spectra

§ Present address: Laboratoire de Biophysique des Transporteurs d'Electrons, Université d'Aix-Marseille II, 163 Avenue de Luminy, 13288 Marseille, Cedex 9, France.

|| E. I. du Pont de Nemours & Co.

[1] Abbreviations: PS II, photosystem II; RC, reaction center; Tyr_D, tyrosine D2-160; Tyr_Z, tyrosine D1-161; P_{680}, primary chlorophyll electron donor of PS II.; Q_A, primary electron acceptor plastoquinone; Chl, chlorophyll; *p*-cresol, *p*-methylphenol; Mes, 2-(*N*-morpholino)-ethane sulfonic acid; $^2H_4$-Tyr, tyrosine with deuterated ring; $^{13}C_6$-Tyr, tyrosine with all six ring carbons ^{13}C-labeled; $^{13}C_1$(4)-Tyr, tyrosine, ^{13}C-labeled at the ring C4 carbon binding the hydroxyl group; ν (δ), stretching (bending) vibration; FTIR, Fourier transform infrared; RR, resonance Raman; ESEEM, electron spin−echo envelope modulation.

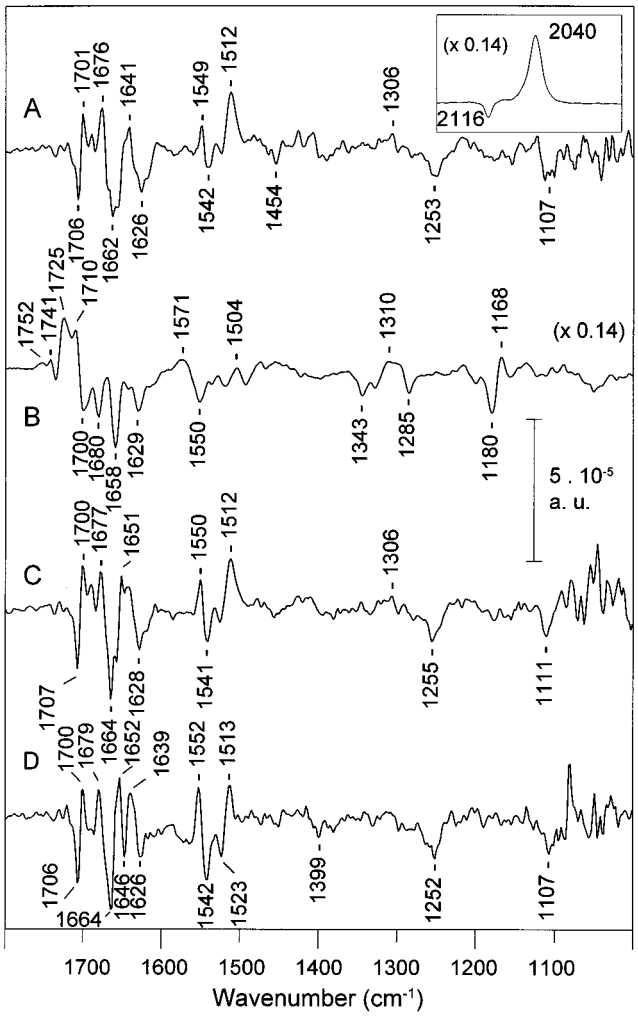

FIGURE 1: $Tyr_Z^{\bullet}/Tyr_Z$ FTIR difference spectra (A) recorded with PS II core complexes from the *Synechocystis* D2-Tyr160Phe mutant, 12 7460 scans (inset: 2100−1900 cm^{-1} region of spectrum A), (C) recorded with core particles of WT *Synechocystis* sp. PCC 6803 grown in the presence of unlabeled aromatic amino acids, 18 7060 scans, and (D) recorded on Mn-depleted PS II-enriched membranes of spinach, 21 800 scans. (B) $P_{680}Chl^+/P_{680}Chl$ FTIR difference spectrum recorded under continuous illumination with PS II core complexes from the *Synechocystis* D2-Tyr160Phe mutant, 2800 scans; 265 K, 4 cm^{-1} resolution.

obtained with isolated PS II RC and PS II-enriched membranes of spinach, respectively. This spectrum is characterized notably by large positive bands at 1725 and 1710 cm^{-1} and by negative ones at 1700, 1680, and 1180 cm^{-1}, which are absent in Figure 1A. Therefore, we conclude that contributions from Chl^+ in Figure 1A remain negligible and spectrum A is denoted $Tyr_Z^{\bullet}/Tyr_Z$. Recently, $Tyr_Z^{\bullet}/Tyr_Z$ and $Tyr_D^{\bullet}/Tyr_D$ FTIR difference spectra have been published (*40*), which largely differ from the data presented here and in refs *26*, *27*, and *41*. These spectra are very similar to Q_A^-/Q_A spectra, and the sign of the ferricyanide band actually indicates that they result from dominant contributions from the electron acceptor side of PS II (*40*).

Spectrum C in Figure 1 was recorded under the same experimental conditions as described for spectrum A with PS II cores of WT *Synechocystis* sp. PCC 6803 grown in the presence of aromatic amino acids. Spectrum C is highly similar to that in Figure 1A. It is thus concluded that it is possible to record a $Tyr_Z^{\bullet}/Tyr_Z$ FTIR spectrum free of contributions from $Tyr_D^{\bullet}$ in WT PS II at pH 6 and also that the D2-Tyr160Phe mutation does not affect the environment of Tyr_Z and $Tyr_Z^{\bullet}$ (in contrast with data in ref *42*). The characteristic features of the $Tyr_Z^{\bullet}/Tyr_Z$ FTIR difference spectrum are a differential signal at 1707/1700 cm^{-1}, a positive signal at 1512 cm^{-1}, and negative ones at 1664−1662, 1628−1626, 1542, 1255−1253, and 1111−1107 cm^{-1} (Figure 1, panels A and C). The $Tyr_Z^{\bullet}/Tyr_Z$ FTIR difference spectrum recorded on Mn-depleted PS II-enriched membranes of spinach is shown in Figure 1D. This signal is very similar to those obtained for *Synechocystis* sp. PCC 6803. All the characteristic features are observed, at frequencies within 1−3 cm^{-1}. The only difference consists of the presence of a negative signal at 1646 cm^{-1} in Figure 1D.

The $Tyr_Z^{\bullet}/Tyr_Z$ (Figure 1, panels A, C, and D) and $Tyr_D^{\bullet}/Tyr_D$ FTIR difference spectra (Figure 3B; *26*, *27*) also show a number of similar features.[2] These spectral features appear in general at slightly higher frequencies in the $Tyr_Z^{\bullet}/Tyr_Z$ spectrum than in the $Tyr_D^{\bullet}/Tyr_D$ spectrum, in particular at 1706/1700 (1702/1696), 1628−1626 (1624), 1523 (1521), 1512 (1503), and 1255−1253 (1250) cm^{-1}. It was shown previously that some of the signals in the $Tyr_D^{\bullet}/Tyr_D$ FTIR difference spectrum arise from IR side chain modes of Tyr_D and $Tyr_D^{\bullet}$ (*27*, *41*). In particular, negative signals at 1275 and 1250 cm^{-1} have been assigned to the $\nu_{7a'}$(CO) and δ-(COH) modes of Tyr_D, and the positive signal at 1503 cm^{-1} has been assigned to the ν(CO) mode of the radical $Tyr_D^{\bullet}$ (*27*).

IR Modes of Tyr_Z and $Tyr_Z^{\bullet}$. To identify the IR side chain modes of Tyr_Z and $Tyr_Z^{\bullet}$, we compare in Figure 2A−C the $Tyr_Z^{\bullet}/Tyr_Z$ FTIR spectra obtained with PS II cores from *Synechocystis* sp. PCC 6803 grown in the presence of aromatic amino acids with unlabeled Tyr (thin line) or with $^{13}C_1$(4)-Tyr (spectrum A, bold line), $^{13}C_6$-Tyr (spectrum B, bold line), or $^2H_4$-Tyr (spectrum C, bold line). Two signals in the $Tyr_Z^{\bullet}/Tyr_Z$ FTIR spectrum are clearly influenced by the ^{13}C-labeling of the Tyr C4 ring carbon (Figure 2A): the positive signal at 1512 cm^{-1} is downshifted by 27 cm^{-1} to 1485 cm^{-1}, and the negative band at 1255 cm^{-1} in the spectrum thin line is strongly reduced and seems downshifted to ≈1234 cm^{-1} in the spectrum obtained in the presence of $^{13}C_1$(4)-Tyr (Figure 2A, bold line). Since the $^{13}C_1$(4)-Tyr labeling influences mostly IR vibrations implicating the C4−O bond of Tyr and $Tyr^{\bullet}$ (*27*, *43*), we can assign the positive band at 1512 cm^{-1} to the ν(CO) mode of $Tyr_Z^{\bullet}$. The shift by 27 cm^{-1} is very close to that of 29 cm^{-1} observed for the 1513 cm^{-1} band of $Tyr^{\bullet}$ obtained by UV irradiation in vitro (*43*). By analogy with the study performed on Tyr_D and the model compound, *p*-methylphenol (*27*), the negative signal observed at 1255 cm^{-1} in the $Tyr_Z^{\bullet}/Tyr_Z$ FTIR difference spectrum, is proposed to account for the δ(COH) mode of Tyr_Z. The corresponding signal for $^{13}C_1$(4)-Tyr_Z is not entirely clear (in Figure 2A bold line) but appears as a broad signal at ≈1234 cm^{-1} as revealed in the calculated double-difference spectrum between spectra of Figure 2A

[2] The $Tyr_Z^{\bullet}/Tyr_Z$ spectra have a signal-to-noise lower than the $Tyr_D^{\bullet}/Tyr_D$ spectra. The fast disappearance kinetics of $Tyr_Z^{\bullet}$ and the 1-s delay between illumination and the FTIR spectrum acquisition (to avoid IR contributions from Q_A^-/Q_A) explain that Tyr_Z/Tyr_Z signals are measured in only 15−20% of the PS II centers. Also, the decay kinetics of $Tyr_Z^{\bullet}$ could be faster in our concentrated PS II sample than that determined by the UV−Vis experiment (*32*).

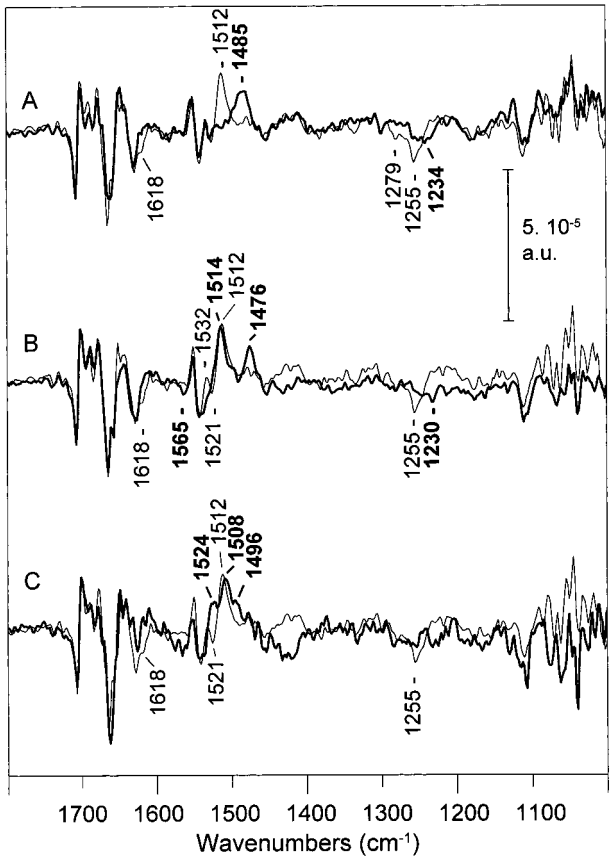

FIGURE 2: Superposition of the $Tyr_Z^{\bullet}/Tyr_Z$ FTIR difference spectrum recorded on PS II core complexes from the *Synechocystis* WT grown in the presence of aromatic amino acids (spectra thin line) and WT grown on (A) $^{13}C_1(4)$-Tyr, bold line, 172 400 scans; (B) $^{13}C_6$-Tyr, bold line, 150 760 scans; (C) $^2H_4$-Tyr, bold line, 200 800 scans; 4 cm^{-1} resolution.

thin and bold line (data not shown). A small negative band at 1279 cm^{-1} in Figure 2A is consistently affected by the $^{13}C_1(4)$-Tyr labeling. Although the signal-to-noise is lower than that obtained for $Tyr_D^{\bullet}/Tyr_D$ spectra, we propose that the band at 1279 cm^{-1} might account for the $\nu_{7a'}$(CO) mode of Tyr_Z, by analogy with that observed at 1275 cm^{-1} for Tyr_D (*27*).

In the $Tyr_Z^{\bullet}/Tyr_Z$ spectrum recorded with PS II samples with $^{13}C_6$-Tyr, a new positive band appears at 1476 cm^{-1} (Figure 2B, bold line) while the positive band at 1532 cm^{-1} in spectrum thin line is altered. The signal of spectrum thin line at 1512 cm^{-1} identified as the $Tyr_Z^{\bullet}$ ν(CO) mode by its sensitivity to Tyr $^{13}C_1(4)$-labeling is also expected to downshift by 35−40 cm^{-1} upon $^{13}C_6$-Tyr labeling (*27*, *43*, *44*). Therefore, the positive band at 1476 cm^{-1} in Figure 2 spectrum (bold line) is assigned to the ν(CO) mode of $^{13}C_6$-labeled $Tyr_Z^{\bullet}$. The positive band at 1514 cm^{-1} thus results from the shift of a mode at higher frequency, probably the mode giving rise to the signal at 1532 cm^{-1} in the unlabeled sample. The large amplitude of the 1514 cm^{-1} band in Figure 2 (bold line) as compared to that of the signal at 1532 cm^{-1} in spectrum thin line may be due to overlap between the positive 1532 cm^{-1} band and a negative band at ≈1520 cm^{-1} in spectrum thin line. The positive band at 1532 cm^{-1} is tentatively assigned to a ring ν(CC) mode of $Tyr_Z^{\bullet}$, probably equivalent to that observed at 1533−1532 cm^{-1} for $Tyr_D^{\bullet}$ (*27*). A positive signal was also observed at 1513 cm^{-1} in the $Tyr_D^{\bullet}/Tyr_D$ spectrum obtained in the presence of $^{13}C_6$-Tyr (*27*).[3] The negative signal at 1255 cm^{-1} in spectrum B (thin line) is downshifted upon $^{13}C_6$-Tyr labeling to ≈1230 cm^{-1} (spectrum B-bold line). This shift is consistent with its assignment to the δ(COH) mode of Tyr_Z, as discussed above. A negative signal at 1521 cm^{-1} in the absorption region of the Tyr ν_{19}(CC) mode seems perturbed by $^{13}C_6$-Tyr labeling, but the corresponding mode of $^{13}C_6$-Tyr expected around 1480 cm^{-1} is not clearly observed in Figure 2 spectrum bold line.

The presence of IR modes of the $Tyr_Z^{\bullet}$ side chain at 1532 and 1512 cm^{-1} and of the Tyr_Z side chain at 1255 cm^{-1} in the $Tyr_Z^{\bullet}/Tyr_Z$ spectrum are confirmed by the sensitivity of these signals to Tyr $^2H_4$-labeling (Figure 2C). The positive bands at 1532 and 1512 cm^{-1} in the thin line spectrum seem downshifted by 24 and 16 cm^{-1} to 1508 and 1496 cm^{-1}, respectively, upon Tyr $^2H_4$-labeling (spectrum 2C bold line). Also, a negative signal at 1618 cm^{-1} in the $Tyr_Z^{\bullet}/Tyr_Z$ spectrum appears sensitive to all Tyr labelings (Figure 2). This band is tentatively assigned to the ν_{8a}(CC) mode of Tyr_Z, although spectra obtained with Tyr in vitro indicate that this mode should only be slightly affected by $^{13}C_1(4)$-labeling (−5 cm^{-1}; *27*). The assignments proposed for Tyr_Z and $Tyr_Z^{\bullet}$ side chain modes based on the isotope shifts are summarized in Table 1 Section A, and compared to the IR modes of Tyr_D.

Figure 3 shows the FTIR spectra corresponding to tyrosyl radical formation in PS II and in vitro. Spectrum A is the $Tyr_D^{\bullet}/Tyr_D$ spectrum obtained with the D2-His189Gln PS II mutant, and spectrum B is the $Tyr_D^{\bullet}/Tyr_D$ spectrum obtained with WT PS II of *Synechocystis* sp. PCC 6803 (*27*). Spectrum C is the $Tyr_Z^{\bullet}/Tyr_Z$ spectrum of Figure 1C. Spectrum D shows the $Tyr^{\bullet}$/Tyr FTIR spectrum obtained by UV irradiation of 10 mM Tyr in borate buffer at pH 12, and spectrum E is the S_3'/S_2' spectrum obtained upon illumination of Ca^{2+}-depleted PS II membranes in the presence of ferricyanide (*45*). The latter spectrum corresponds to the formation of the split EPR signal centered at $g \approx 2$, which was shown to result from the magnetic interaction between an organic radical and the Mn cluster in the $S = 1/2$ spin state (*46*).[4] It was recently shown that this radical is sensitive to Tyr $^2H_4$-labeling and hence proposed to be due to $Tyr_Z^{\bullet}$ (*6*). Indeed, several features of spectrum 3E are common with those of the $Tyr_Z^{\bullet}/Tyr_Z$ spectrum (Figure 3C), in particular with that recorded with Mn-depleted PS II-enriched membranes (Figure 1D). These are the differential signal at 1705(1706)/1700 cm^{-1}, signals of the amide I and amide II regions at 1678(1679)/1665(1664), 1651(1652), and 1552/1540(1542) cm^{-1}, negative bands at 1402(1399) and 1110-(1107) cm^{-1}, and the positive signal at 1514 (1513) cm^{-1}. Infrared bands only present in the S_3'/S_2' spectrum are the positive band at 1447 cm^{-1} and a sharp differential signal at 1659/1655 cm^{-1} in the amide I region. The bold frequencies noted in Figure 3 represent the ν(CO) mode of the tyrosyl

[3] The data obtained for $Tyr_Z^{\bullet}/Tyr_Z$ suggest that both for $Tyr_D^{\bullet}$ and $Tyr_Z^{\bullet}$ the ν(CC) mode at 1534−1532 cm^{-1} may be actually downshifted to 1513−1514 cm^{-1} upon $^{13}C_6$-Tyr labeling, in contrast to the previous assignment proposed in ref *27*.

[4] The split signal and the resulting loss of the hyperfine line of the multiline signal due to the magnetic interaction were both simulated (*47*). The distance between the radical and the Mn cluster was estimated between 6 and 12 Å from the value of the dipolar and exchange coupling constants (*48*).

Table 1

Section A: Isotope-Sensitive IR Modes of Tyr_Z and $Tyr_Z^•$ Side Chains[a]

	Tyr_Z	$^{13}C_1(4)$-Tyr_Z	$^{13}C_6$-Tyr_Z	$^2H_4$-Tyr_Z	Tyr_D
ν_{8a}(CC)	1618		1565 (−53)	1595 (−22)	1615
ν_{19}(CC)	1521			1482 (−44)	1513−1510
$\nu_{7'a}$(CO)	1279			1233 (−22)	1275
δ(COH)	1255	1234	1230		1250
	$Tyr_Z^•$	$^{13}C_1(4)$-$Tyr_Z^•$	$^{13}C_6$-$Tyr_Z^•$	$^2H_4$-$Tyr_Z^•$	$Tyr_D^•$
ν_{8a}(CC)	1532		1514 (−18)	1508 (−24)	1533−1532
ν(CO)	1512	1485 (−27)	1476 (−36)	1496 (−16)	1503

Section B: ν(CO) IR Mode of $Tyr^•$ Radicals

		$Tyr_D^•$		$Tyr_Z^•$			
	$Tyr^•$ (RR)[b]	D2-189Gln	WT PS II	WT PS II	spinach	S3′ spinach	*in vitro*
ν(CO)	1498	1497	1503	1512	1513	1514	1513

[a] The frequencies are obtained from the double-difference spectra calculated from the unlabeled *minus* labeled difference spectra of Figure 2. [b] Resonance Raman data on ribonucleotide reductase from ref *60*.

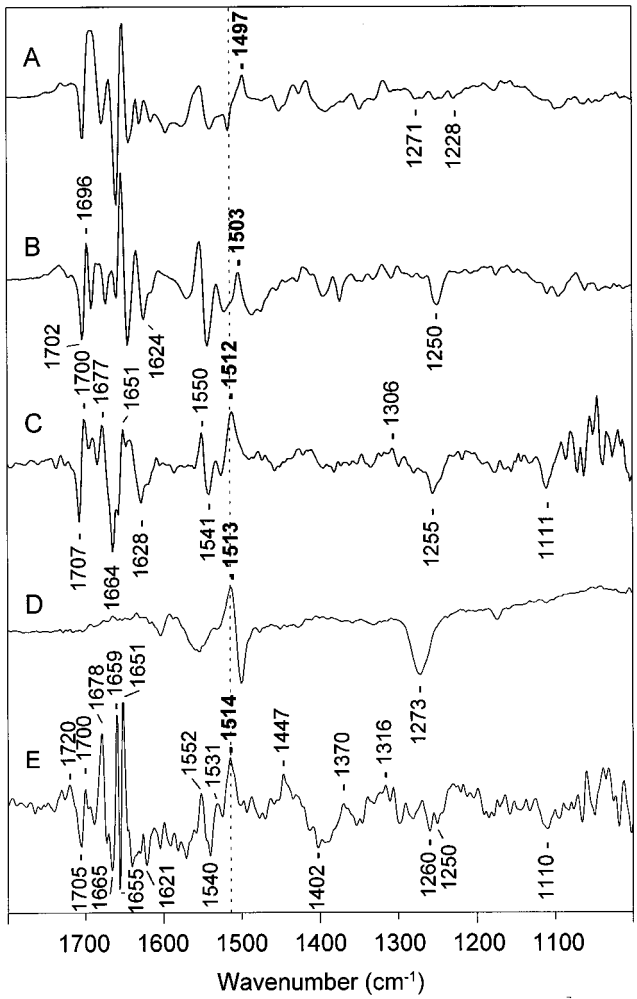

FIGURE 3: Light-induced FTIR difference spectra (A) $Tyr_D^•/Tyr_D$ in PS II core complexes from the *Synechocystis* D2-His189Gln mutant, 138 640 scans; (B) $Tyr_D^•/Tyr_D$ in PS II core complexes from the *Synechocystis* WT, 107840 scans; (C) $Tyr_Z^•/Tyr_Z$ in PS II core complexes from the *Synechocystis* WT; (D) $Tyr^•/Tyr$ obtained at 10 K by a 2-s UV irradiation (with a 1000 W Hg−Xe Oriel lamp) of a 10 mM solution of Tyr in borate buffer at pH 12, 2560 scans. It was shown by NMR that interactions between Tyr molecules remain negligible at this concentration. (E) S_3'/S_2' in Ca^{2+}-depleted PS II-enriched membranes of spinach (*45*).

radicals, identified by isotope labeling for Figure 3, panels A−C, and proposed to contribute at 1514 cm^{-1} in the S_3'/S_2' spectrum of Figure 3E.

DISCUSSION

$Tyr_Z^•/Tyr_Z$ spectra free of contributions from Q_A^-/Q_A and Chl^+/Chl signals have been obtained both with Mn-depleted PS II cores of *Synechocystis* sp. PCC 6803 and PS II-enriched membranes of spinach. For *Synechocystis*, a signal at 1255 cm^{-1}, sensitive to specific isotope labeling, is assigned to the δ(COH) mode of Tyr_Z side chain by comparison with literature data and with the studies performed for Tyr_D and for *p*-cresol in different solvents (ref *27* and references therein). Another mode at 1279 cm^{-1}, consistently observed in several independent spectra, is proposed to account for the $\nu_{7'a}$(CO) mode of Tyr_Z. We have shown previously for *p*-cresol that the frequencies and the relative intensities of the $\nu_{7'a}$(CO) and δ(COH) IR modes are determined by the interactions formed by *p*-cresol and its environment (*27*). The $\nu_{7'a}$(CO) and δ (COH) modes of Tyr_D at 1275 and 1250 cm^{-1} were in agreement with the presence of a strong hydrogen bond between Tyr_D and the neutral imidazole side chain of histidine. The analogy observed between the frequency and intensity of the $\nu_{7'a}$(CO) and δ(COH) modes of Tyr_D and Tyr_Z leads us to propose that Tyr_Z is also hydrogen bonded to the neutral side chain of a histidine, probably D1-His190 (*13*, *22*, *23*). Kinetic arguments have also implicated D1-His190 as the acceptor of the phenolic proton upon Tyr_Z oxidation (*20*, *21*). All the side chain modes appear at slightly higher frequencies for Tyr_Z than for Tyr_D. In particular, frequency differences of +4 and +5 cm^{-1} are observed for the $\nu_{7'a}$(CO) and δ(COH) modes, respectively (Table 1). A frequency upshift of the $\nu_{7'a}$(CO) mode of *p*-cresol in different solvents is observed upon an increase of the hydrogen acceptor character of the solvent molecule(s) (*27*, *49*). Therefore, the +4 cm^{-1} frequency difference observed between Tyr_Z and Tyr_D indicates that the hydroxyl group of Tyr_Z is in a stronger hydrogen acceptor environment than that of Tyr_D. These results are in line with the analysis done on the UV−Vis difference spectra of $Tyr_D^•$ and $Tyr_Z^•$ formation by Candeias et al. (*50*), who proposed that the hydroxyl of reduced Tyr_Z is implicated in a strong hydrogen bond. The δ(COH) mode of Tyr_Z is slightly broader than that of Tyr_D. Indeed shoulders appear at ≈1260 and ≈1246 cm^{-1} in the $Tyr_Z^•/Tyr_Z$ spectrum (Figure 2A, thin line), which could be due to the $\nu_{7'a}$(CO) and δ(COH) modes of a different population of Tyr_Z in a minority of PS II centers. These frequencies suggest that these Tyr_Z would

also be hydrogen bonded either to water or to hydroxylated amino acid side chains or to the protonated imidazole side chain of histidine ($HisH_2^+$ instead of HisH; *27*). The study of pH effects on the $Tyr_Z^•/Tyr_Z$ spectra should help discriminate between these possibilities.

For the radical $Tyr_Z^•$, the ν(CO) mode is unambiguously assigned at 1512 cm^{-1} by $^{13}C_1$(4)-Tyr labeling and comparison with IR and resonance Raman (RR) studies of UV-induced radicals of $^{13}C_1$(4)-Tyr, ^{16}O-, ^{18}O-*p*-cresol•, and ^{18}O- or ^{17}O-phenoxyl in vitro (*43, 44*).[5] The effect of $^{13}C_6$- and $^2H_4$-Tyr labeling on the $Tyr_Z^•/Tyr_Z$ spectra also suggests that a second mode of $Tyr_Z^•$ contributes at 1532 cm^{-1}. In RR spectra of para-substituted phenoxyl radicals, a mode is observed at 1556−1577 cm^{-1} (*44, 55*−*57*). This mode, unaffected by ^{17}O-labeling of phenoxyl (*44*) is assigned to the vibrations mainly at the ring $C_{ortho}-C_{para}$ bonds and denoted ν_{8a}(CC). Although the signal observed at 1532 cm^{-1} for $Tyr_Z^•$ appears at lower frequency than that reported at 1565 cm^{-1} by RR for Tyr• in solution (*57*), we propose that it corresponds to the ν_{8a}(CC) mode of $Tyr_Z^•$. This signal is close to that observed for $Tyr_D^•$ at 1533−1532 cm^{-1} (*27*) in WT PS II. The frequency and intensity of this mode is sensitive to interactions such as coordination to different metals (*58*). This mode is not observed for $Tyr_D^•$ in the D2-His189Gln mutant and for UV-induced Tyr• radical in solution (*27, 43, 59*). For $Tyr_D^•$, it was shown by EPR and cw- and pulsed-ENDOR that a hydrogen bond exists to the side chain of D2-His189 (*15*−*17*). Therefore, we speculate that the enhancement of the signal at 1532 cm^{-1} for $Tyr_D^•$ in WT PS II is due to the hydrogen bond with the imidazole side chain of D2-His189. By analogy, we propose that $Tyr_Z^•$ is also hydrogen bonded by the side chain of a histidine, probably that of D1-His190 (*13, 22, 23*). Based on kinetic experiments in site-directed mutants (*20, 21*), D1-His190 has been proposed as the acceptor of the phenoxyl proton upon $Tyr_Z^•$ formation. This close interaction would lead one to expect, as in the case of $Tyr_D^•$ and D2-His189, back hydrogen bonding of D1-His190 to $Tyr_Z^•$.

The ν(CO) mode of $Tyr_Z^•$, at 1512 cm^{-1}, is higher by 9 cm^{-1} than that of $Tyr_D^•$ in WT PS II. It is higher by 14 cm^{-1} than that of $Tyr_D^•$ in the D2-His189Gln mutant for which it was shown that $Tyr_D^•$ is not hydrogen bonded (*15*−*17*). On the other hand, the frequency of the ν(CO) mode of $Tyr_Z^•$ is very similar to that of the Tyr• formed by UV irradiation in solution (1513 cm^{-1}), where Tyr• is hydrogen bonded to water molecule(s) (Table 1, Section B, see also data obtained by RR, at 1510 cm^{-1}, in ref *57*). On the basis of these data and also from the ν(CO) mode of the non-hydrogen-bonded tyrosyl radical of ribonucleotide reductase reported at 1498 cm^{-1}, by resonance Raman (*60*), we propose that the ν(CO) mode of Tyr• radicals is upshifted upon formation of hydrogen bond(s). Thus, $Tyr_Z^•$ would form a hydrogen bond with the protein comparable to that formed by Tyr• in water and stronger than that formed by $Tyr_D^•$ with D2-His189 in WT PS II (*17*). Alternatively, the frequency difference observed between the ν(CO) modes of $Tyr_D^•$ and $Tyr_Z^•$ could be explained, besides the presence of a hydrogen bond (to His) by greater positive charge in the immediate vicinity of the phenoxyl oxygen of $Tyr_D^•$ than of $Tyr_Z^•$. Indeed, resonance Raman data on Zn-coordinated substituted phenoxyl radicals show that the ν(CO) mode of the phenoxyl is largely affected by the total charge of the metal−ligand complexes (*58, 61*). The binding of phenoxyl to Zn(II), with 0 total charge of the complex induces a +9 cm^{-1} upshift of the ν(CO) mode of the phenoxyl, from ≈1511 to 1520 cm^{-1}. Upon +1 and +2 charge increase of the Zn complexes, however, the frequency of this ν(CO) mode decreases by 10 and 16 cm^{-1}, respectively. The same tendency is observed for the Cu(II) complexes but with smaller amplitude (*62*). Greater positive charge in the immediate vicinity of the phenoxyl oxygen of $Tyr_D^•$ than of $Tyr_Z^•$ could be due to the greater polarity of the environment of $Tyr_Z^•$ or to a larger proton release associated with the oxidation of Tyr_Z than Tyr_D. The former would be consistent with the greater accessibility of the Tyr_Z environment to solvent water (Diner, unpublished; *5*) and the observation that in acetate-treated PS II the number of water molecules in the vicinity of $Tyr_D^•$ and $Tyr_Z^•$ could be different (*63*). Another interpretation is that D1-His190 may be a transient but not the final proton acceptor upon $Tyr_Z^•$ formation. The location of the positive charge upon $Tyr_Z^•$ formation is still a matter of debate (*32, 64, 65*).

$Tyr_Z^•$ and $Tyr_D^•$ have been studied by high field EPR and by comparison with the Tyr• of ribonucleotide reductase (*19*). It was concluded from the g_x component of the anisotropic *g*-tensor for the two EPR spectra that the tyrosyl radicals of WT PS II are both hydrogen bonded, in contrast to the Tyr• of ribonucleotide reductase and $Tyr_D^•$ in the D2-His189Gln mutant PS II. The frequency of the ν(CO) IR mode of Tyr• shows a correlation similar to that of the g_x edge of the high field EPR spectra. The difference between the high field EPR spectra of $Tyr_Z^•$ and $Tyr_D^•$ is the breadth of the g_x edge for $Tyr_Z^•$, interpreted as the existence of a multiplicity of different environments around $Tyr_Z^•$. Such a heterogeneity in hydrogen bonding of $Tyr_Z^•$ is consistent with spectral features assigned to hydrogen bonding in pulsed ENDOR (*1, 18*). If we assume a strict correlation between the value of the g_x component and the ν(CO) mode frequency in infrared, we would expect similar frequencies for $Tyr_Z^•$ and $Tyr_D^•$, which is not the case. The signal obtained at 1512 cm^{-1} for $Tyr_Z^•$ is slightly broader than that at 1503 cm^{-1} for $Tyr_D^•$ (*27, 41*), with a width at half heigth of ≈13 and ≈9 cm^{-1}, respectively. The ν(CO) mode of $Tyr_Z^•$ is nonetheless a well-defined peak that appears at significantly higher frequency than for $Tyr_D^•$ (+9 cm^{-1}).

For Mn-depleted PS II-enriched membranes of spinach, we propose that the ν(CO) mode of $Tyr_Z^•$ contributes at 1513 cm^{-1} (Figure 1D). The question remains of a possible influence of Mn depletion on the environment of Tyr_Z in PS II. In the presence of Mn but in Ca^{2+}-depleted PS II, it was shown that illumination induces the formation of a S_2-Tyr• state (*6*), and it was proposed that this Tyr• is $Tyr_Z^•$. The spectral analogies between the spectrum of $Tyr_Z^•/Tyr_Z$ in Mn-depleted PS II of spinach and the so-called S_3'/S_2' FTIR spectrum (Figure 3D; *45*) are in favor of this assign-

[5] The ν(CO) mode of all phenoxyl and tyrosyl radicals reported in the literature lies between 1520 and 1487 cm^{-1}. The frequencies that we identify at 1512 cm^{-1} for $Tyr_Z^•$ and at 1503−1498 cm^{-1} for $Tyr_D^•$ in WT and mutant PS II are in this range. In contrast, the ν(CO) mode proposed at 1478 cm^{-1} for $Tyr_Z^•$ and $Tyr_D^•$ in (*40, 51*−*53*) is significantly below this range. The present study, with others (*26, 27, 33*−*37, 41*), should clarify the ongoing controversy (*40, 54*) concerning the assignment of Q_A^-/Q_A, $Tyr_D^•/Tyr_D$, and $Tyr_Z^•/Tyr_Z$ FTIR difference spectra in PS II.

ment. We propose that the ν(CO) mode of $Tyr_Z^\bullet$ contributes at 1514 cm^{-1} in the Ca^{2+}-depleted, Mn-containing PS II (Figure 3D). Both in Mn-containing and Mn-depleted PS II, the IR frequency of this mode is very similar. Also, the ν(CO) mode of $Tyr_Z^\bullet$ has the same width in both cases. Thus it seems that, at least as viewed by FTIR, Mn removal does not induce perturbations of the immediate environment of $Tyr_Z^\bullet$ phenoxyl. Noguchi et al. (*41*) report infrared modes of Tyr_Z side chain in the S_2/S_1 spectrum recorded with PS II cores of *Synechocystis* sp. PCC 6803 which they attribute to an interaction between Tyr_Z and the Mn cluster. The signals identified at 1521 and 1254 cm^{-1} for Tyr_Z in the S1 state are in agreement with our assignment of side chain modes of Tyr_Z at 1255 and possibly at 1521 cm^{-1} in Mn-depleted PS II. However, one concern is the possible contamination of the S_2/S_1 spectrum by IR signals due to $Tyr_Z^\bullet$ formation in a fraction of PS II centers lacking intact Mn cluster. In particular, the difference signal at 1707/1698 cm^{-1} observed only in the S_2/S_1 spectrum recorded with PS II cores from *Synechocystis* (*41*) is similar to that at 1707/1700 cm^{-1} in the $Tyr_Z^\bullet/Tyr_Z$ spectrum. The signal at 1707-(1705)/1700 cm^{-1} is observed in both the $Tyr_Z^\bullet/Tyr_Z$ and S_3'/S_2' spectra (Figures 1D and 3D). It appears at higher frequency than a similar signal of the $Tyr_D^\bullet/Tyr_D$ spectrum, at 1702/1696 cm^{-1}. This signal is the only IR difference signal of the $Tyr_Z^\bullet/Tyr_Z$ spectrum identified in the $Tyr_Z^\bullet Q_A^-/Tyr_Z Q_A$ spectrum recorded by Zhang et al. (*37*) due to the dominance of overlapping signals of the Q_A^-/Q_A spectrum. This difference signal appears in the absorption region of carbonyl groups, either from the polypeptide backbone or from the chlorophyll cofactors. For $Tyr_D^\bullet/Tyr_D$, it was proposed that this signal might reflect changes of the 9-keto carbonyl vibration of a Chl of PS II upon $Tyr_D^\bullet$ formation (*26*, *27*) in agreement with the presence of a large infrared mode at 1700 cm^{-1} in the FTIR spectrum corresponding to P_{680} and/or Chl oxidation in PS II (Figure 1B; *38*). This vibrational change could be a response to the charge that gives rise to the electrochromic shift observed in the visible range (*32*). This interpretation has also been proposed for the $Tyr_Z^\bullet Q_A^-/Tyr_Z Q_A$ spectrum (*37*). However, equally probable is that the difference signals correspond to the shift of a peptide carbonyl, for example, at Tyr_Z and Tyr_D amide group, respectively. In this respect, the higher frequency observed for the difference signal in the $Tyr_Z^\bullet/Tyr_Z$ spectrum as compared to $Tyr_D^\bullet/Tyr_D$, would correlate with the higher frequency observed for the side chain modes of Tyr_Z as compared to Tyr_D.

In conclusion, we have identified infrared modes of Tyr_Z and $Tyr_Z^\bullet$ in the Mn-depleted PS II cores of *Synechocystis* sp. PCC 6803. The frequency of the ν(CO) mode of $Tyr_Z^\bullet$, as compared to that of $Tyr_D^\bullet$ and of tyrosyl radical in solution suggests either that $Tyr_Z^\bullet$ forms stronger hydrogen bond(s) with its environment than $Tyr_D^\bullet$ or that a more localized positive charge exists around the phenoxyl oxygen of $Tyr_D^\bullet$. That the FTIR of the split signal is very similar to $Tyr_Z^\bullet/Tyr_Z$ in the Mn-depleted core complexes indicates that the environment of $Tyr_Z^\bullet$, as viewed by FTIR, is essentially the same with and without Mn. We are currently investigating the pH effects on $Tyr_Z^\bullet/Tyr_Z$ FTIR spectra to better understand the interaction between $Tyr_Z^\bullet$ and its environment.

REFERENCES

1. Force, D. A., Randall, D. W., Britt, R. D., Tang, X.-S., and Diner, B. A. (1995) *J. Am. Chem. Soc. 117*, 12643−12644.
2. Gilchrist, M. L., Ball, J. A., Randall, D. W., and Britt, R. D. (1995) *Proc. Natl. Acad. Sci. U.S.A. 92*, 9545−9549.
3. Hoganson, C. W., Lydakis-Simantiris, N., Tang, X.-S., Tommos, C., Warncke, K., Babcock, G. T., Diner, B. A., MaCracken, J., and Styring, S. (1995) *Photosynth. Res. 46*, 177−184.
4. Tommos, C., Tang, X.-S., Warncke, K., Hoganson, C. W., Styring, S., McCracken, J., Diner, B. A., and Babcock, G. T. (1996) *J. Am. Chem. Soc. 117*, 10325−10335.
5. Babcock, G. T., Espe, M., Hoganson, C., Lydakis-Simantiris, N., McCracken, J., Shi, W., Styring, S., Tommos, C., and Warncke, K. (1997) *Acta Chem. Scand. 51*, 533−540.
6. Tang, X.-S., Randall, D. W., Force, D. A., Diner, B. A., and Britt, R. D. (1996) *J. Am. Chem. Soc. 118*, 7638−7639.
7. Diner, B. A., and Babcock, G. T. (1996) Structure, Dynamics, and Energy conversion efficiency in Photosystem II in *Oxygenic photosynthesis: the light reactions*. Advances in Photosynthesis Vol. 4, pp 213−247, Kluwer, Dordrecht. (Ort, D. R., and Yocum, C. F., Eds.)
8. Boussac, A., and Etienne, A.-L. (1984) *Biochim. Biophys. Acta 766*, 576−581.
9. Vass, I., and Styring, S. (1991) *FEBS Lett. 226*, 347−351.
10. Rodriguez, I. D., Chandrashekar, T. K., and Babcock, G. T. (1987) in *Progress in Photosynthesis Research* (Biggins, J., Ed.) pp 471−474, Martinus Nijhoff, Dordrecht.
11. Debus, R. J., Barry, B. A., Babcock, G. T., and MacIntosh, L. (1988) *Proc. Natl. Acad. Sci. U.S.A. 85*, 427−430.
12. Evelo, R. G., Hoff, A. J., Dikanov, S. A., and Tyrishkin, A. M. (1989) *Chem. Phys. Lett. 161*, 479−484.
13. Svensson, B., Vass I., Cedergren, E., and Styring, S. (1990) *EMBO J. 7*, 2051−2059.
14. Mino, H., Satoh, J.-I., Kawamori, A., Toriyama, K., and Zimmerman, J.-L. (1993) *Biochim. Biophys. Acta 1144*, 426−433.
15. Tang, X.-S., Chisholm, D. A., Dismukes, G. C., Brudwig, G. W., and Diner, B. A. (1993) *Biochemistry 32*, 13742−13748.
16. Tommos, C., Davidson, L., Svensson, B., Madsen, C., Vermaas, W. F. J., and Styring, S. (1993) *Biochemistry 32*, 5436−5441.
17. Campbell, K. A., Peloquin, O. M., Diner, B. A., Tang, X.-S., Chrisholm, D. A., and Britt, R. D. (1997) *J. Am. Chem. Soc. 119*, 4787−4788.
18. Tang, X.-S., Zheng, M., Chisholm, D. A., Dismukes, G. C., and Diner, B. (1996) *Biochemistry 35*, 1475−1484.
19. Un, S., Tang, X.-S., and Diner, B. A. (1996) *Biochemistry 35*, 679−684.
20. Diner, B. A., Nixon, P. J., and Farchaus, J. W. (1991) *Curr. Opin. Struct. Biol. 1*, 546−554.
21. Hays, A. M., A., Vasiliev, I. R., Golbeck, J. H., and Debus, R. J. Submitted.
22. Ruffle, S. V., Donnelly, D., Blundell, T. L., and Nugent, J. H. A. (1992) *Photosynth. Res. 34*, 287−300.
23. Svensson, B., Etchebest, C., Tuffery, P., van Kan, P., Smith, J., and Styring, S. (1996) *Biochemistry 35*, 14486−14502.
24. Mäntele, W. (1993) *Trends Biochem. Sci. 18*, 197−202.
25. Siebert, F. (1993) in *Methods in Enzymology, Biochemical Spectroscopy* (Sauer, K., Ed.) Vol. 246, pp 501−526, Academic Press, San Diego.
26. Hienerwadel, R., Boussac, A., Breton, J., and Berthomieu, C. (1996) *Biochemistry 35*, 15447−15460.
27. Hienerwadel, R., Boussac, A., Breton, J., Diner, B., and Berthomieu, C. (1997) *Biochemistry 36*, 14712−14723.
28. Rögner, M., Nixon, P. J., and Diner, B. A. (1990) *J. Biol. Chem. 265*, 6189−6196.
29. Williams, J. G. K. (1988) *Methods Enzymol. 167*, 766−778.
30. Rippka, R., Deruelles, J., Waterbury, J. B., Herdman, M., and Stanier, R. Y. (1979) *J. Gen. Microbiol. 111*, 1−61.
31. Barry, B. A., and Babcock, G. T. (1987) *Proc. Natl. Acad. Sci. U.S.A. 84*, 7099−7103.
32. Diner, B. A., Tang, X.-S., Zheng, M., Dismukes, G. C., Force, D. A., Randall, D. W., and Britt, R. D. (1995) in *Photosyn-*

thesis: from Light to Biosphere (Mathis, P., Ed.) Vol. II, pp 229−234, Kluwer Academic Publishers, Dordrecht.
33. Berthomieu, C., Nabedryk E., Mäntele W., and Breton J. (1990) *FEBS Lett. 269*, 363−367.
34. Berthomieu C., Nabedryk, E., Breton, J., and Boussac, A. (1992) in *Research in Photosynthesis* (Murata, N., Ed.) Vol. II, pp 53−56, Kluwer Academic Publishers, Dordrecht.
35. Noguchi, T., Ono, T., and Inoue, Y. (1992) *Biochemistry 31*, 5953−5956.
36. Araga, C., Akabori, K., Sasaki, J., Maeda, A., Shrina, T., and Toyoshima, Y. (1993) *Biochim. Biophys. Acta 1142*, 36−42.
37. Zhang, H., Razeghifard, M. R., Fischer, G., and Wydrynski, T. (1997) *Biochemistry 36*, 11762−11768.
38. Breton, J., Hienerwadel, R., and Nabedryk, E. (1997) in *Spectroscopy of Biological Molecules: Modern Trends* (Carmona, P., Navarro, R., and Hernanz, A., Eds.) pp 101−102, Kluwer Academic Publishers, Dordrecht.
39. Noguchi, T., and Inoue, Y. (1995) *FEBS Lett. 370*, 241−244.
40. Kim, S., and Barry, B. A. (1998) *Biophys. J. 74*, 2588−2600.
41. Noguchi, T., Inoue, Y., and Tang, X.-S. (1997) *Biochemistry 36*, 14705−14711.
42. Boerner, R. J., Bixby, K. A., Nguyen, A. P., Nore, G. H., Debus, R., and Barry, B. A. (1993) *J. Biol. Chem. 268*, 17151−17154.
43. Berthomieu, C., Boullais, C., Neumann, J.-M., and Boussac, A. (1998) *Biochim. Biophys. Acta 1365*, 112−116.
44. Mukherjee, A., McGlashen, M. L., and Spiro, T. G. (1995) *J. Phys. Chem. 99*, 4912−4917.
45. Berthomieu, C., and Boussac, A. (1995) *Biochemistry 34*, 1541−1548.
46. Boussac, A., Zimmermann, J.-L., and Rutherford, A. W. (1989) *Biochemistry 28*, 8984−8989.
47. Boussac, A., Zimmermann, J.-L., Rutherford, A. W., and Lavergne, J. (1990) *Nature 347*, 303−306.
48. Zimmermann, J.-L., Boussac, A., and Rutherford, A. W. (1993) *Biochemistry 32*, 4831−4841.
49. Takeuchi, H., Watanabe, N., Satoh, Y., and Harada, I. (1989) *J. Raman Spectrosc. 20*, 233−237.
50. Candeias, L. P., Turconi, S., and Nugent, J. H. A. (1998) *Biochim. Biophys. Acta 1363*, 1−5.
51. MacDonald, G. M., and Barry, B. A. (1992) *Biochemistry 31*, 9848−9856.
52. MacDonald, G. M., Bixby, K. A., and Barry, B. A. (1993) *Proc. Natl. Acad. Sci. U.S.A. 90*, 11024−11028.
53. Bernard, M. T., MacDonald, G. M., and Barry, B. A.(1995) *J. Biol. Chem. 270*, 1589−1594.
54. McDonald, G. M., Steenhuis, J., and Barry, B. A. (1995) *J. Biol. Chem*. 270, 8420−8428.
55. Tripathi, G. N. R., and Schuler, R. H. (1988) *J. Phys. Chem. 92*, 5129−5133.
56. McGlashen, M. L., Eads, D. D., Spiro, T. S., and Whittaker, J. W. (1995) *J. Phys. Chem. 99*, 4918−4922.
57. Johnson, C. R., Ludwig, M., and Asher, S. A. (1986) *J. Am. Chem. Soc. 108*, 905−912.
58. Schnepf, R., Sokolowski, A., Müller, J., Bachler, V., Wieghardt, K., and Hildebrandt, P. (1998) *J. Am. Chem. Soc. 120*, 2352−2364.
59. Berthomieu, C., and Boussac, A. (1995) *Biospectroscopy 1*, 187−206.
60. Backes, G., Sahlin, M., Sjöberg, B.-M., Loehr, T. M., and Sanders-Loehr, J. (1989) *Biochemistry 28*, 1923−1929.
61. Sokolowski, A., Müller, J., Weyhermüller, T., Schnepf, R., Hidebrandt, P., Hildebrand, K., Bothe, E., and Wieghardt, K. (1997) *J. Am. Chem. Soc. 119*, 8889−8900.
62. Sokolowski, A., Leutbecher, H., Weyhermüller, T., Schnepf, R., Bothe, E., Bill, E., Hidebrandt, P., and Wieghardt, K. (1997) *JBIC, J. Biol. Inorg. Chem. 2*, 444−453.
63. Force, D. A., Randall, D. W., and Britt, R. D. (1997) *Biochemistry 36*, 12062−12070.
64. Rappaport, F., and Lavergne, J. (1997) *Biochemistry 36*, 15294−15302.
65. Ahlbrink, R., Haumann, M., Cherepanov, D., Bögershausen, O., Mulkidjanian, A., and Junge, W. (1998) *Biochemistry 37*, 1131−1142.

BI980788M